Nationaal Lucht- en Ruimtevaartlaboratorium
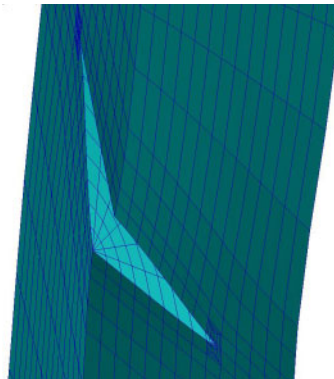
National Aerospace Laboratory NLR

Executive summary

Stress intensity factors and crack propagation in a single crystal nickel-based superalloy

Fracture surface and finite element model of single crystal test specimen

Problem area

To improve gas turbine efficiency the turbine inlet temperatures have steadily increased. One way to meet the increasing demands on materials used is the application of single crystal materials. In modern jet engines single crystal materials are used for the turbine blades and vanes. As part of component life assessment the material fatigue crack propagation behaviour must be modelled. The major differences for the crack growth analysis of single crystal materials compared to the polycrystalline case are the anisotropic material behaviour and the crack growth on crystallographic slip planes.

Description of work

In this paper methods are developed to predict crack propagation in single crystal materials. Firstly finite element (FE) analyses are performed to calculate the stress intensity factors for a single crystal test specimen. Both the material anisotropy and the possibility of an angled crack are taken into account. Secondly a method is developed to predict the direction of crack propagation in single crystal materials, based on the material orientation and loading direction. Using this approach, the fatigue crack growth behavior in single crystal corner cracked specimens can be explained.

This report is based on an article published in Engineering Fracture Mechanics 73 (2006) by Elsevier.

Results and conclusions

Comparison of the results learned that the use of the calculated anisotropic stress intensity factor solutions yields a more accurate prediction of crack propagation than the use of the isotropic handbook solutions. Also, it is shown that the experimentally observed direction of crack growth can be predicted using the method presented in this paper.

Applicability

The tools presented in this paper can be used to assist gas turbine operators in maintenance and life assessment issues. For example, the length of inspection intervals or the specified service life can be judged. Further, the tools can also be applied to generate crack propagation characteristics during failure analyses on single crystal components.

NLR-TP-2006-358

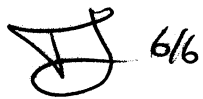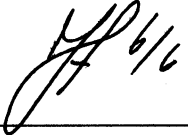# Stress intensity factors and crack propagation in a single crystal nickel-based superalloy

T. Tinga

Customer	National Aerospace Laboratory NLR
Contract number	---
Owner	National Aerospace Laboratory NLR
Division	Aerospace Vehicles
Distribution	Unlimited
Classification of title	Unclassified

Approved by:

Author	Reviewer	Managing department
6/6	6/6	7/6

Summary

This report contains a research article that was published in Engineering Fracture Mechanics, 73 (2006), pp.1679-1692. The original paper that was submitted to the journal in October 2005 was published in NLR-TP-2005-470. Since the final paper has undergone some major revisions, it is now published in a separate report. The technical content of the paper is summarized in the abstract.

Contents

Stress intensity factors and crack propagation in a single crystal nickel-based superalloy

Tiedo Tinga[*]

National Aerospace Laboratory NLR, Anthony Fokkerweg 2, 1059 CM, Amsterdam, The Netherlands

Abstract

A 3-dimensional finite element method was used to calculate the stress intensity factors for corner cracked specimens of a single crystal nickel-based superalloy. The anisotropic material properties and inclinations of the cracks were shown to have significant effects on the stress intensities. Then the 2-dimensional resolved shear stress approach for predicting the crack planes and crack growth directions in single crystals was extended to the 3-dimensional case. Using this approach, the fatigue crack growth behaviour in single crystal corner cracked specimens could be explained.

Keywords: Stress intensity factor; single crystal; anisotropy;

1 Introduction

To improve gas turbine efficiency the turbine inlet temperatures have steadily increased. This makes greater demands on the materials used for the turbine rotor blades and stator vanes. One way to meet these demands is to use single crystal materials. In modern jet engines single crystal materials are used for the turbine blades and vanes.

As part of component life assessment the material fatigue crack propagation behaviour must be modelled. Two major differences exist for the crack growth analysis of single crystal materials compared to the polycrystalline case. Firstly the material behaviour is anisotropic, which results in different stress and deformation fields around the crack tip. Secondly, cracks propagate along distinct crystallographic planes, which means they are often angled cracks not on a plane normal to the major principal stress, unlike cracks in isotropic materials.

To model single crystal crack propagation behaviour the anisotropic stress intensity factors should be determined for both normally-oriented and angled cracks. Many studies have been done on the fracture mechanics of anisotropic materials, both on bulk materials [1-6] and notched geometries [7,8]. The earlier papers [1-3,5,6] mainly focus on 2-dimensional cases and analytical approaches, whereas the more recent work [7-10] directs towards 3-dimensional cases and numerical methods. However, still anisotropic stress intensity factor solutions are usually not available. Therefore it has often been assumed, or shown for specific materials [1,2,4], that the differences between isotropic and anisotropic solutions are negligible and that the isotropic solution can be used. Similarly, it has been assumed [2,4] that the standard stress intensity factor solutions for normally-oriented cracks can be used for angled cracks, provided the angles made with the normal plane are small.

[*] Corresponding author. Tel.: +31-527-248727; fax: +31-527-248210. *Email address:* tinga@nlr.nl

Nomenclature

a, a$_{cr}$	crack length
a, b, c	material orientation angles in analysis tool
a$_{ij}$	material constitutive matrix
ΔK	stress intensity factor range
E	Young's modulus
FCC	face centred cubic (crystal lattice)
FE	finite element
G	shear modulus
K, K$_I$, K$_{II}$, K$_{III}$	stress intensity factors (modes I, II and III)
K$_{eff}$	effective stress intensity factor
K$_{rss}$	resolved shear stress intensity parameter on slip system
LEFM	linear elastic fracture mechanics
r	distance to crack tip
S	remotely applied stress
SIF	Stress Intensity Factor
t	specimen width
T	projected specimen width
α, β	crack orientation angles in analysis tool
β	geometrical correction function for SIF
ε	strain
μ$_i$	roots of characteristic equation
ν	Poisson's ratio
σ	stress
τ$_{rss}$	resolved shear stress
θ	angle with respect to the normal crack plane

The first objective of the present work is to show that standard stress intensity factor solutions cannot be used for the anisotropic nickel-based superalloy CMSX-4 and angled cracks. The second objective is to extend to 3 dimensions the 2-dimensional resolved shear stress method [1,3,4,11] for predicting the crack planes and crack growth directions in single crystals.

2 Isotropic and anisotropic stress intensity factors

The basis of linear elastic fracture mechanics (LEFM) theory is the stress intensity factor (SIF or K) concept, which relates the local elastic stress field near the crack tip to the known global stress or displacement field. Relations for the stress intensity factor can be derived by calculating the stress or displacement field, in the crack tip local coordinate frame, as functions of the distance r and angle θ, see Figure 1. The stress field in a small region surrounding the crack tip is given by [5,12]

$$\sigma_i(r,\theta) = \frac{1}{\sqrt{2\pi r}}\left[K_I f_i(\mu,\theta) + K_{II} g_i(\mu,\theta) + K_{III} h_i(\mu,\theta)\right] \qquad (i = 1...6)$$

(1)

In this relation f_i, g_i and h_i are geometrical functions defining the angular dependency of the stress field, and K$_I$, K$_{II}$ and K$_{III}$ are the mode I, II and III stress intensity factors. For the anisotropic case the stress field also depends on the roots μ_i of the characteristic equation, which is defined below. In an infinite plate containing a crack with length $2a$ and loaded by a normal stress σ_y and shear stresses τ_{xy} and τ_{yz}, the stress intensity factors are defined as

6

$$K_I = \sigma_y \sqrt{\pi a} \quad ; \quad K_{II} = \tau_{xy} \sqrt{\pi a} \quad ; \quad K_{III} = \tau_{yz} \sqrt{\pi a} \tag{2}$$

For any situation deviating from this ideal situation the value of K is modified by a factor $\beta(a)$, e.g.:

$$K_I = \sigma_y \sqrt{\pi a} \cdot \beta_I(a) \tag{3}$$

The function $\beta(a)$ accounts for geometrical effects like finite width corrections. A number of handbooks are available [13,14] in which the function $\beta(a)$ is supplied for most common problems, but it can also be obtained from a finite element (FE) analysis by comparing the calculated displacement field (which in an FE analysis is more accurate than the stress distribution) with the (theoretical) displacement field around a crack in an infinite plate loaded in plane tension.
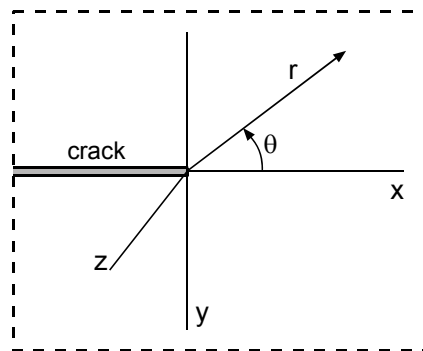

Figure 1 Definition of the variables r and θ and the crack tip local coordinate frame.

For isotropic materials the functions f_i, g_i and h_i can be related directly to the material properties E and v, but for anisotropic materials, they are functions of the complex roots μ_i of the characteristic equation [5]

$$a_{11}\mu^4 - 2a_{16}\mu^3 + (2a_{12} + a_{66})\mu^2 - 2a_{26}\mu + a_{22} = 0 \tag{4}$$

where the coefficients a_{ij} are the (compliance) elements of the elastic constitutive matrix, relating the stresses and strains according to

$$\varepsilon_i = a_{ij}\sigma_j \qquad (i, j = 1...6) \tag{5}$$

For an orthotropic material with cubic symmetry (e.g. a single crystal FCC material), there are only three independent compliances: a_{11} ($= a_{22} = a_{33}$), a_{12} ($= a_{21} = a_{13} = a_{31} = a_{23} = a_{32}$) and a_{44} ($= a_{55} = a_{66}$). All other compliances are zero. This constitutive matrix must be defined in the coordinate frame of the crack (see Figure 1).

In the next section we describe how an FE analysis is used to calculate the anisotropic stress intensity factors for single crystal corner cracked specimens of a nickel-base superalloy.

3 Stress intensity factors for single crystal corner cracked specimens

The commercial finite element code MSC.Nastran was used to calculate the stress intensity factors for single crystal corner cracked specimens of a nickel-base superalloy. MSC.Nastran provides special crack tip elements (CTEs), whose midside nodes are moved to the quarter

positions to better represent the stress field singularity at the crack tip. The calculated stress intensity factors are directly given as element output.

The NLR in-house tool *NLR-C3D* [15] was used to insert an initial crack in an existing finite element model. *NLR-C3D* replaces elements in the mesh by crack blocks, which define the crack plane and locally refine the mesh, see Figure 2. It also inserts the CTEs, six (6) along the crack front in the present case, and automatically calculates stress intensity factors for different crack sizes.
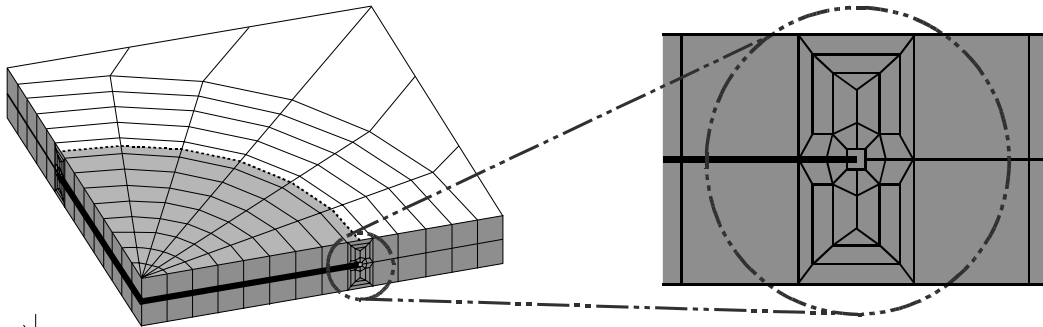

Figure 2   Slice of the FE model near the crack plane and detailed view of crack blocks inserted by the NLR-C3D tool. The crack is indicated by the thick lines and the shaded region in the top face of the body in the left-hand-side figure.
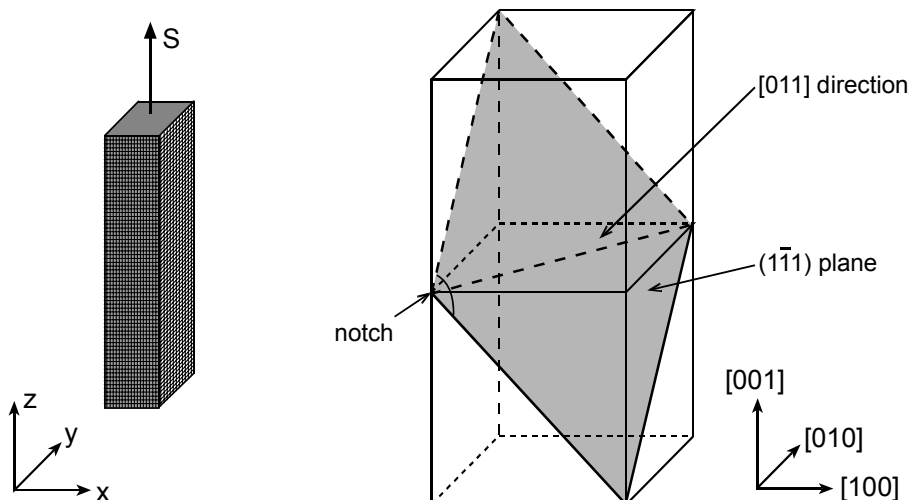

Figure 3 Schematic representation of crystal orientation in test specimen and important crystal directions and planes

Stress intensity factors were calculated for two cases: a corner crack propagating on the plane normal to the applied load, and a corner crack propagating on a 45° plane as shown in Figure 3. The latter case represents the situation in which a crack propagates along a {111}-type plane in a single crystal FCC material aligned with the [001] direction along the tensile axis (*z*-axis), and the [100] and [010] directions along the *x*- and *y*-axes. Since corner cracks are 3-dimensional, the stress intensity factor (SIF) solutions were calculated for six (6) different positions along the crack fronts, corresponding to the angular centres of each CTE. The two FE meshes are shown in Figure 4. These are somewhat more detailed than the meshes used by Pickard [12]. A tensile load was applied in the *z*-direction. The end-faces of the bars were restrained to move in *x*- and *y*-direction to keep them aligned in the loading direction.
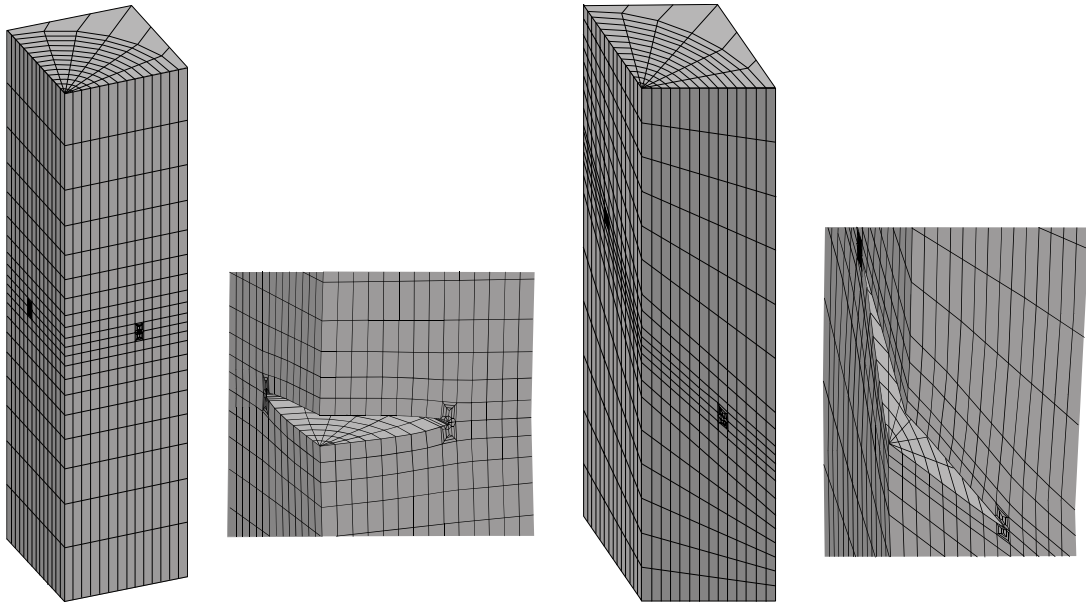
Figure 4 Finite element models for the corner cracked specimen with a crack normal to the tensile axis (left) and a crack under a 45° angle (right).

To quantify the effect of material anisotropy on the stress intensity factors, the SIF values for both the normal and 45° angled cracks were calculated with isotropic and anisotropic material properties. Both the elastic constants and the compliances, as used in equation (4), are given in Table 1.

Table 1   Material properties for Ni-based superalloy.

Property	Isotropic	Orthotropic
E	200 GPa	200 GPa
ν	0.30	0.30
G	76.9 GPa	220 GPa
a_{11}	$5.00 \cdot 10^{-12}$ Pa^{-1}	$5.00 \cdot 10^{-12}$ Pa^{-1}
a_{12}	$-1.50 \cdot 10^{-12}$ Pa^{-1}	$-1.50 \cdot 10^{-12}$ Pa^{-1}
a_{44}	$1.30 \cdot 10^{-11}$ Pa^{-1}	$4.55 \cdot 10^{-12}$ Pa^{-1}

3.1 Normal crack, isotropic properties

The FE model was checked by calculating the corner crack mode I SIFs for a normal crack in an isotropic material and comparing them to the solutions given by Pickard [12] and in an AGARD publication [16]. The results were plotted as a function of the crack length *a* normalised by the

9

specimen width t. Figure 5a shows the comparisons for SIFs along the specimen edges (actually 7.5° from the specimen edges for the MSC.Nastran results): the agreement is generally good to excellent.

Figure 5b compares the edge and centre position SIFs according to Pickard's FE model and the present one. Both models predict higher SIFs along the specimen edges. This difference can be explained by the fact that edge positions are nominally in plane stress, whereas the centre position is nominally in plane strain.
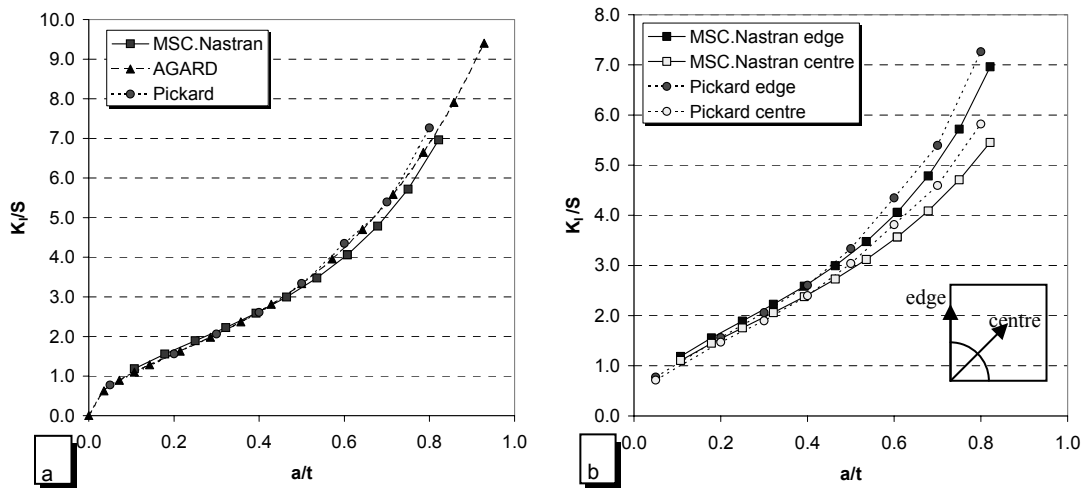

Figure 5 K_I for normal crack and isotropic material: a) comparison of edge solutions and b) showing the difference between a centre and edge position on the crack front.

3.2 Normal crack, orthotropic properties

Figure 6 shows that changing the material properties from isotropic to anisotropic, in the present case orthotropic, more than doubles the K_I values for the normal crack orientation. Also, the difference in K_I between the edge and centre positions is almost the same (factor ~1.3) for both isotropic and orthotropic properties. This is worth noting because in the orthotropic case the elastic properties in the near-<100> directions associated with the crack edge (7.5°) positions are different from those for the near-<110> directions associated with the crack centre (37.5°, 52.5°) positions.

There are two ways in which material anisotropy can affect the value of the stress intensity factor. Firstly, just using the anisotropic method influences the SIF. Secondly, the material anisotropy changes the local stress distribution, which also affects the SIF. Snyder and Cruse [6] concluded that the first effect is quite small (comparing isotropic or anisotropic solutions in the same stress field), but the second effect is much larger. This second effect is automatically included when SIFs are calculated with an FE method, and so Snyder's and Cruse's conclusion is confirmed by the results in Figure 6.
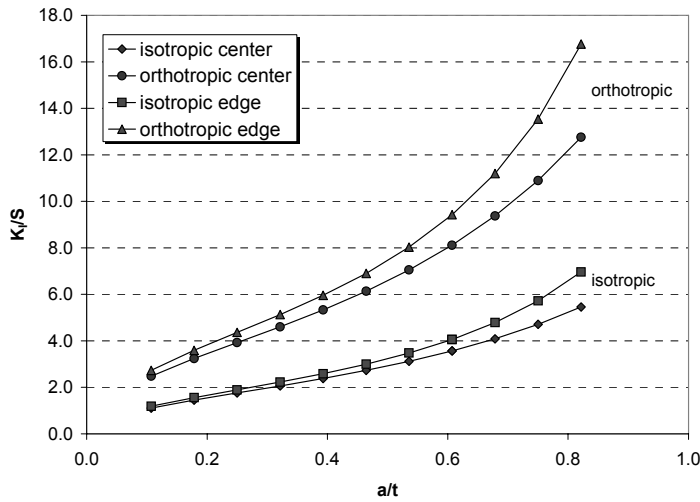
Figure 6 K_I for normal crack, using isotropic and orthotropic material properties.

3.3 Angled crack, isotropic properties

The MSC.Nastran stress intensity factors for an angled crack in an isotropic material are compared with the results of Pickard [12] in Figures 7a and 7b for edge and centre positions, respectively, and are discussed in the following paragraphs.

Figure 7   SIF solutions for 45° angled crack: a) for an edge position (7.5^o), b) for a centre position (37.5^o, 52.5°): note that the abscissa is a/T, where T = t for a normal crack and T = t √2 for a 45° crack.

3.3.1 *(Near) edge positions*

For the edge positions, Figure 7a, the crack plane is tilted 45° about both the *x*- and *z*-axis of the crack tip coordinate frame (Figure 1). This means that all three loading modes are present, with the same magnitude for mod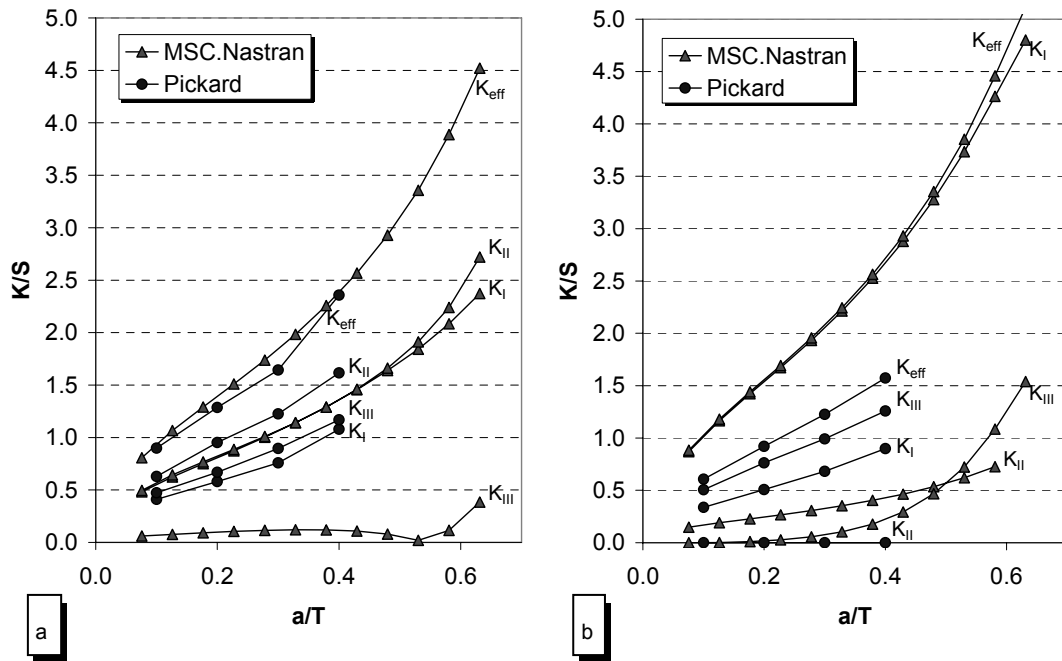e II and III and a slightly smaller magnitude for mode I. Therefore one expects similar K_{II} and K_{III} values and a somewhat smaller K_I value. The MSC.Nastran calculated K_I and K_{II} values are almost identical, but the K_{III} results are significantly lower. This underestimation of K_{III} and overestimation of K_I is caused by the way the CTEs are positioned in the FE model, as will be discussed in section 3.5.
Pickard's data show the expected trends, but the differences between K_I and K_{II} are relatively large and K_{III} is significantly smaller than K_{II}. These differences may be due to the relatively course FE mesh used or due to differently applied boundary conditions, which resulted in the specimen deforming in a less defined way. Nevertheless, the values of K_{eff}, which is the overall driving force for crack growth on the angled plane, and is defined for isotropic materials by

$$K_{eff} = \sqrt{K_I^2 + K_{II}^2 + K_{III}^2}$$

(6)

are fairly similar for the MSC.Nastran and Pickard solutions.

3.3.2 *(Near) centre position*

For the centre position it can be seen from Figure 3 that the crack propagates in a direction normal to the tensile axis but on a plane tilted 45° about the crack tip *x*-axis (Figure 1). Thus the loading is a combination of mode I and III, the latter having the greatest magnitude. One would therefore expect a K_{III} that is somewhat larger than K_I and a negligible K_{II}.
The MSC.Nastran results in Figure 7b do not agree well with these expectations. The relatively low value of K_{III} and the high K_I value are again a result of the positioning of the CTEs in the FE model (see section 3.5). Apparently, the effect of the tilted crack plane is not represented well by the CTEs, so one would expect similar K_I values as for the normal crack. Comparison of the lowest curve in Figure 6 with the uppermost curve in Figure 7b shows that this is indeed the case.
The most likely reason for the non-zero K_{II} is the use of only six CTEs, which means that K values are obtained for near centre (37.5°, 52.5°) positions rather than the exact centre (45°). This is confirmed by the results of an additional analysis, using a refined FE mesh with nine (9) crack tip elements along the crack front. The angular dependency of the three (normalized) SIFs at a specific crack length is shown in Figure 8, which illustrates that at the 45° position K_{II} does become zero.
Pickard's results in Figure 7b show the expected trends, but the low values for K_I and K_{III} are hard to explain. Both the K_I and K_{III} curves are much lower than the MSC.Nastran K_I curve and, as a result, also the K_{eff} curves show a large difference in this case.
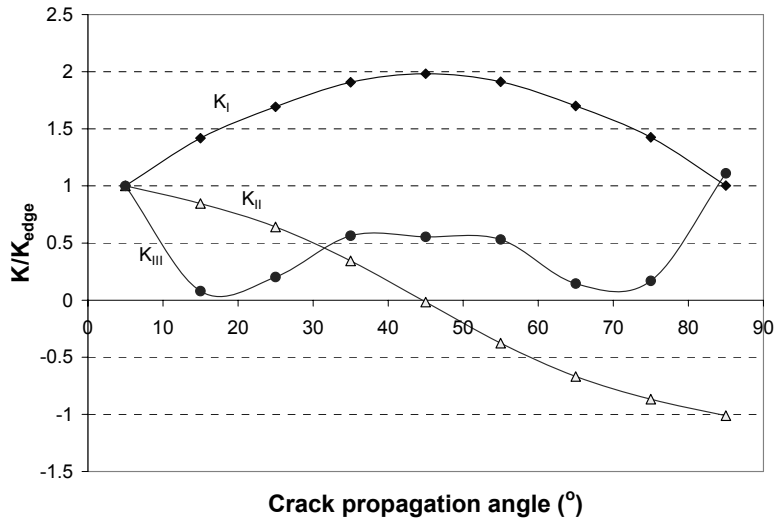
Figure 8   Angular dependency of the SIFs for a 45° angled crack at a/T =0.32. The values of K_I, K_{II} and K_{III} were normalized with the edge K-values (at 5°).

3.3.3   *Angled crack projection approximation*

It is often suggested to approximate the SIFs for an angled crack by using the normal crack SIF solution with the *projected* crack length, i.e. the apparent length of an angled crack when it is projected onto the normal plane. Figure 9 shows that this approximation is invalid for an edge position of a 45° crack, whether one compares the normal crack K_I (= K_{eff}) curve with the angled crack K_I or K_{eff} curves. A similar result will be obtained for the centre position.
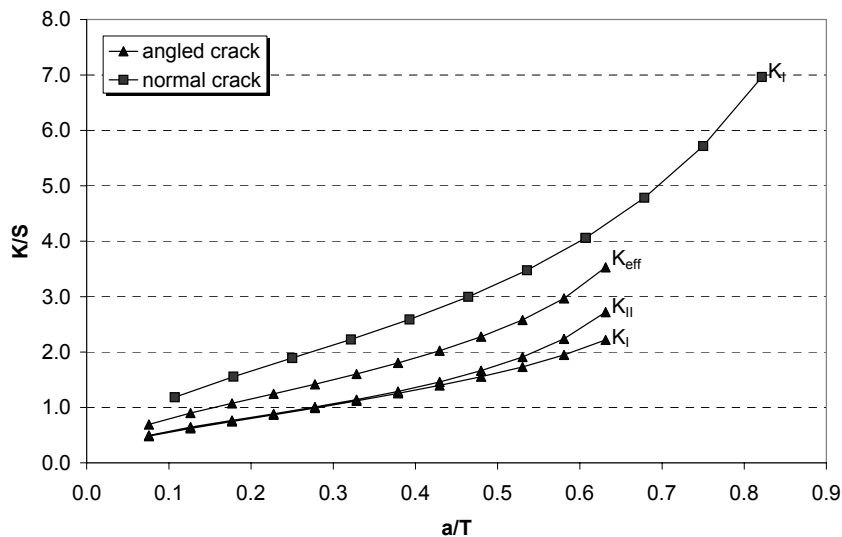

Figure 9   Comparison between normal crack and 45° angled crack for an edge position: note that the abscissa is a/T, where T = t for a normal crack and   T = t √2 for a 45° crack

3.4 Angled crack, orthotropic properties

The calculated results for the angled crack, using orthotropic material properties are shown in Figure 10. It appears from Figure 10a that for an edge position the effect of using orthotropic instead of isotropic properties leads to different SIF solutions, especially for K_{II}. However, both K_I and K_{II} are lower for the orthotropic case, whereas for a normal crack Figure 6 shows that the orthotropic K_I is significantly greater. Figure 10b shows that for a centre position the difference between orthotropic and isotropic stress intensity factors is smaller, especially for K_{II}, but the trends are the same as for an edge position.
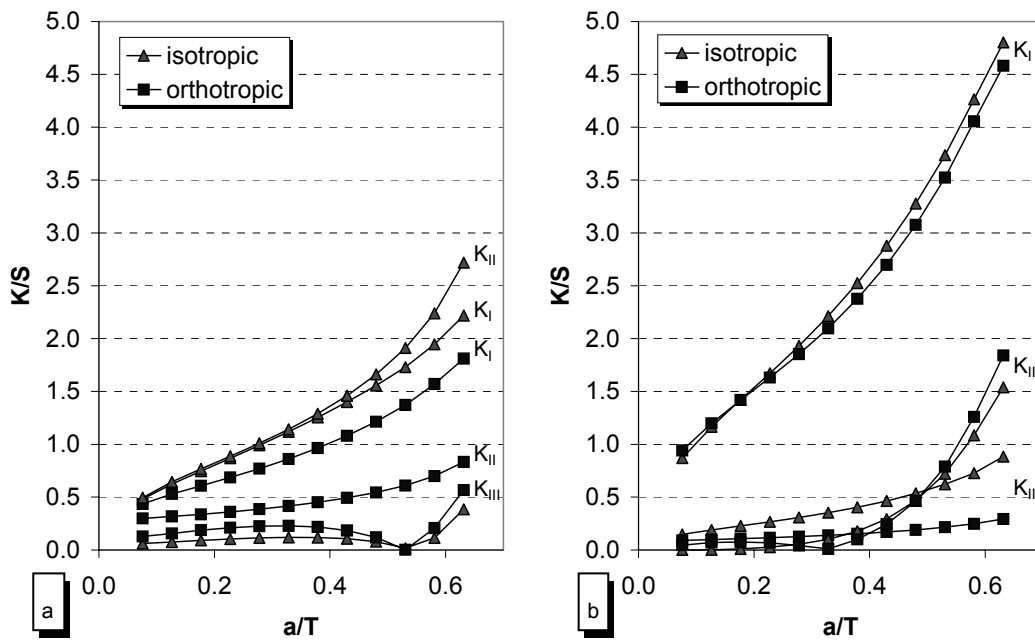

Figure 10   SIF solutions for 45° angled crack. Comparison between isotropic and orthotropic properties for a) edge position and b) centre position: note that the abscissa is a/T, where T = t for a normal crack and T = t √2 for a 45° crack

3.5 Accuracy

The accuracy of the SIF calculations presented in the previous sections is governed by three aspects:
- the method implemented in the MSC.Nastran crack tip elements to calculate the SIFs,
- the coarseness of the finite element mesh,
- the way the CTEs are integrated in the FE model.

The SIFs calculated with MSC.Nastran CTEs are reported [17] to have an accuracy of $2 - 5\%$ compared to theoretical values. The agreement, in Figure 5, between the MSC.Nastran calculated values and two other solutions confirms this. It can further be concluded that the mesh size used in the present models is sufficiently fine to calculate accurate K_I values for a normal crack.

However, these conclusions cannot be unconditionally extended to the calculations for the angled crack case. MSC.Nastran CTEs are hexagonal elements with two faces containing the crack tip and four other faces connecting the crack tip faces (see Figure 11a). The crack tip faces contain 10 nodes each and their displacements are used to resolve the total or effective SIF (K_{eff}) into the K-values for the three different modes. More specifically, the displacements in *x*-, *y*-

and *z*-direction are used to calculate the values of respectively K_{II}, K_I and K_{III}. The coordinate frame used for these calculations should be aligned with the crack plane, as indicated in Figure 1.

In the present model for the angled crack, distorted crack tip elements were used. The crack plane was tilted whereas the faces of the CTEs remained vertical as shown schematically in Figure 11b. Consequently, the crack tip faces of the CTE were not normal to the crack plane of the CTE. Moreover, MSC.Nastran appeared to align the crack tip coordinate frame with the crack tip faces (frame *xyz* in Figure 11b) in stead of the crack plane (frame *x'y'z'*). This resulted in a different division of the effective SIF over the three modes, yielding an overestimated K_I and an underestimated K_{III}. This explains the very low K_{III} values in Figures 7 and 10 and also partly explains the large difference between the MSC.Nastran and Pickard's K_I values in Figure 7b. Only at larger crack lengths, when the model deformed significantly, displacements normal to the crack tip faces appeared and non-zero K_{III} values were calculated. The crack tip *x*-axis is equal in both coordinate frames so the K_{II} values are calculated correctly, as is the total or effective SIF.
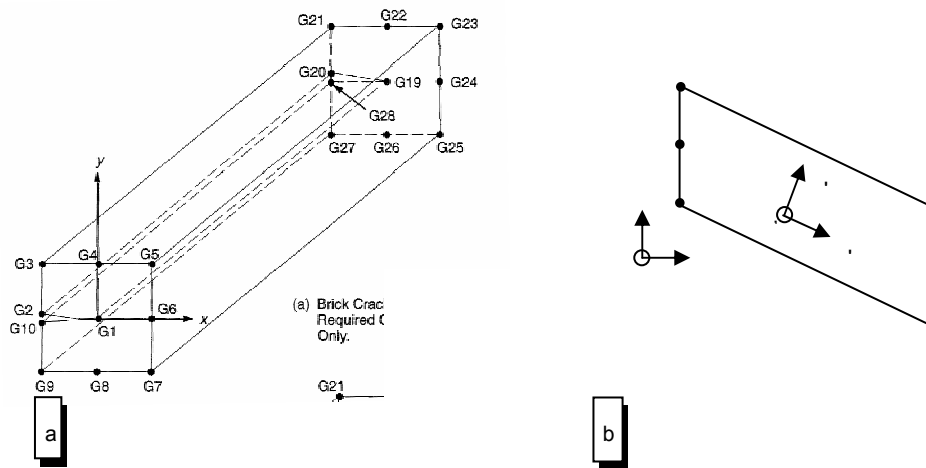

Figure 11 a) MSC.Nastran crack tip element (CTE) with the grid points located in the two crack tip faces. b) side-view of a distorted CTE using the crack tip coordinate frame xyz in stead of x'y'z'.

4 Resolved shear stress intensity parameter

The crack planes and propagation directions in single crystals cannot be predicted from the stress field alone, since cracking is restricted to distinct crystallographic planes. Telesman and Ghosn [1] and Chen and Liu [3] presented a 2-dimensional prediction method based on a resolved shear stress intensity parameter that represents the stress intensity on a specific crystallographic plane. The resolved shear stress intensity parameter is defined as

$$K_{rss} = \lim_{r \to 0} \tau_{rss} \sqrt{2\pi r} \qquad (7)$$

where the value of τ_{rss} is obtained by Schmid-decomposition of the stress tensor to a specific slip system. The limiting value of K_{rss} is obtained by calculating several values near the crack tip and extrapolating to r = 0. Crack propagation will occur on the slip plane with the highest value of K_{rss}.

As stated in section 2, calculations of SIF values with an FE method are most accurate when they are based on displacements. However, a displacement vector cannot be projected to a slip

system. to obtain the resolved shear stress. Telesman and Ghosn [1] calculated K_{rss} from a 2-dimensional reconstructed stress field around the crack tip of an isotropic material, using a boundary integral equation method.

In the present work the stress tensor was reconstructed from the 3-dimensional anisotropic (orthotropic) FE calculations of SIF values for specific situations, together with equation (1). Use of equation (1) requires choosing values of θ. The most obvious choice is the angle between the slip plane (*possibly* destined to become the new crack plane) and the plane normal to the tensile axis, as was done by Telesman and Ghosn [1].

The K_{rss} calculation was incorporated into an analysis tool that requires the following information:

(1) The elastic properties (E, G and v for the <100> cube directions) of the material.

(2) SIF values (K_I, K_{II} and K_{III} for the appropriate orthotropic material and crack orientation) at certain crack lengths, as calculated with the FE model shown in the previous section.

(3) The crystallographic orientation of the material with respect to the specimen coordinate frame. This is specified by three angles (*a*, *b* and *c*), which define the rotation around the specimen *x*-, *y*- and *z*-axes, respectively.

(4) The orientation of the original crack plane with respect to the specimen coordinate frame. This is specified by another two angles (α and β), which define the rotation of the crack plane around the Specimen *x*- and *y*-axes.

The analysis tool then calculates K_{rss} for every slip plane and finds the maximum value. The corresponding slip plane determines the plane and directions of subsequent crack growth. This can be done for any material orientation and any crack orientation.

Table 2 Originally normal crack ideal situation ($a = b = c = 0$, $\alpha = \beta = 0$, $a_{cr} = 1.5$ mm).

Position	K_{rss}	Active slip systems	Subsequent crack angle
Edge 1	1.30	$(111)[0\bar{1}1]$, $(1\bar{1}\bar{1})[01\bar{1}]$	-45°
(y-z plane)	1.30	$(1\bar{1}1)[011]$, $(11\bar{1})[0\bar{1}\bar{1}]$	$+45^o$
Centre	1.47	$(111)[0\bar{1}1]$	-54.7^o
	1.47	$(11\bar{1})[0\bar{1}\bar{1}]$	$+54.7^o$
Edge 2	1.30	$(111)[0\bar{1}1]$, $(1\bar{1}1)[011]$	-45°
(x-z plane)	1.30	$(\bar{1}\bar{1}\bar{1})[01\bar{1}]$, $(11\bar{1})[0\bar{1}\bar{1}]$	$+45^o$

More specifically, for the present work the analysis tool was used to predict the planes and directions of crack propagation in the corner cracked specimens described in section 3. The predictions are compared in subsections 4.1-4.3 with representative experimental results for fatigue crack growth in single crystal CMSX-4 specimens [18].

4.1 Original crack normal to tensile axis, perfect crystallographic alignment

When the original crack plane is normal to the tensile axis ($\alpha = \beta = 0$) and the crystallographic alignment of the specimen is perfect ($a = b = c = 0$) there are four slip systems with the same K_{rss}. This is illustrated in Table 2 for an arbitrary original crack length of 1.5 mm: the K_{rss} value of 1.30 for the Edge 1 position shows that subsequent crack propagation is likely at both -45° and $+45^o$ to the tensile axis. The first column in Table 2 specifies the position along the original crack front, where the mentioned coordinate planes refer to Figure 3.

16

4.2 Original +45° crack, perfect crystallographic alignment

In this second example the original crack was at +45° to the tensile axis. Starting with an edge length of only 0.1 mm, the predictions were that the crack stays on the original slip plane until at least 0.5 mm length. This is shown in the first row of Table 3. However, when the crack becomes larger than 0.5 mm it is predicted to switch to the -45° slip plane, see the second row in Table 3.

Table 3 Originally +45° angled crack (a = b = c = 0, α = 45°, β = 0).

Position	K_{rss}	Active slip systems	Subsequent crack angle
Edge 1 - a_{cr} = 0.5 mm	0.655	$(1\bar{1}1)[011]$	+45°
Edge 1 - a_{cr} = 0.6 mm	0.621	$(111)[0\bar{1}1]$	-45°

After some amount of crack growth, the same process will cause the crack to switch back to the +45° slip plane. In fact, what actually happens is that a crack grows in a zig-zag fashion, alternating between +45° and -45° and remaining macroscopically in the plane normal to the tensile axis. This was observed for specimen A of the experimental programme [18], see figure 12a, although the alignment for this specimen was not perfect. This is discussed further in subsection 4.3.
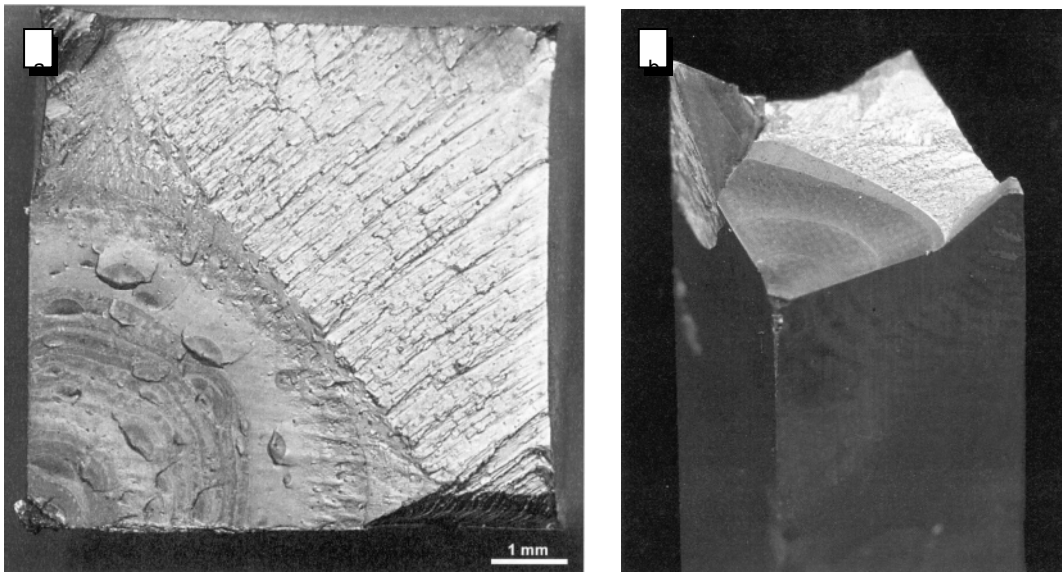
Figure 12 a) fracture surface in corner cracked specimen A. The crack front is macroscopically normal to the tensile axis. b) specimen B fracture surface, showing the transition from normal to angled crack plane. Both photographs from [18].

4.3 Original +45°crack, imperfect crystallographic alignment

If the crystallographic alignment of the specimen is imperfect, there should be a preference for crack growth on one slip plane. Then, since the crack does not switch to another slip plane, a macroscopically angled crack develops.
Using the K_{rss} approach the misalignment behaviour was analysed for a +45° original crack and five simple crystallographic misalignments, whereby a = 3°, 5°, 7°, 10°, and 15°, and b = c = 0. Starting with an edge crack length of 0.1 mm, the predictions were that all cracks stay on the

original slip plane until lengths of 1.1 - 4.5 mm, depending on the misalignment, see Table 4. These crack lengths are significantly larger than the 0.5 mm for a perfectly aligned specimen (see Table 3) and as the misalignment increases there is eventually no change of slip plane. This means that the crack grows in a zig-zag fashion until the crack length is reached where no transition to another slip plane is possible anymore. Table 4 shows that for small misalignments (a ~ 3° - 5°) there is no such crack length and for large misalignments (a ~ 10° - 15°) this crack length is zero, indicating that an angled crack develops from the beginning. For intermediate misalignments there is a crack length at which the crack switches, but there is also a length above which no switching can occur anymore.

Thus a macroscopically normal crack can develop in two situations:

(1) perfect crystallographic alignment: a zig-zag crack develops because switching is not bounded by a certain crack length.

(2) intermediate misalignment: the bounding crack length at which the zig-zag crack transitions into an angled crack is beyond the crack length at failure.

The data in Table 4 enable explaining the fatigue crack growth behaviour of the specimens shown in Figure 12. Specimen A had a primary crystallographic misalignment of 8.5^o and also a considerable secondary misalignment of c = 8° [18]. Crack growth occurred in a zig-zag fashion, Figure 10a. This is an example of an intermediate misalignment with a transition to an angled crack beyond the crack length at failure. However, specimen B had a primary misalignment a = 7.3° and only a slight secondary misalignment. This resulted in one transition from the normal crack plane to an angled crack plane at an edge crack length of 3.8 mm, see the L.H. edge in Figure 12b. The transition crack lengths agree reasonably with the predictions in Table 4.

Since the two specimen edges are in perpendicular planes, a crystallographic misalignment in a specific direction has a different effect on the crystallographic orientation of the material at each of the two edges. This explains the small differences in crack propagation along the specimen edges in Figure 12.

Table 4 Crack lengths at which preferred direction changes from +45o to -450 for different material orientations (b = c = 0, α = 45o, β = 0).

Position	a = 3°	a = 5°	a = 7°	a = 10°	a = 15°
Edge 1	1.4 mm	2.2 mm	4.5 - 6.5 mm[a]	no change	no change
Edge 2	0.0 mm	1.1 mm	1.6 - 3.7 mm[a]	2.1 - 3.3 mm[a]	no change

[a] preferred direction changes to -45° at first crack length, but is again +45° for cracks larger than the second crack length (= no subsequent change beyond this crack length).

5 Concluding remarks

This study has shown that for single crystals of a nickel-base superalloy, CMSX-4, it is inappropriate to use isotropic stress intensity factor solutions, and also projected crack lengths for angled cracks. However, anisotropic stress intensity factor solutions incorporated into a 3-dimensional stress tensor reconstruction, followed by calculations of the resolved shear stress intensity factor, K_{rss} , gave predictions that explain the fatigue crack growth behaviour in single crystal CMSX-4 corner cracked specimens.

The approach in the present work is based on finite element analyses. This means that it can be extended to the more complex geometries of actual gas turbine components (e.g. single crystal turbine blades and vanes). An efficient crack propagation method, based on the calculation of a

closed form stress intensity factor solution and K_{rss}, is under development and will be published in a future paper.

6 Acknowledgements

References

[1] Telesman J. and Ghosn L. J. The unusual near-threshold FCG behaviour of a single crystal superalloy and the resolved shear stress as the crack driving force. Engineering Fracture Mechanics 1989;34(5/6):1183-1196.

[2] Chan K. S. and Cruse T. A. Stress intensity factors for anisotropic compact-tension specimens with inclined cracks. Engineering Fracture Mechanics 1986;23(5):863-874.

[3] Chen, Q. and Liu, H. W. Resolved shear stress intensity coefficient and fatigue crack growth in large crystals. CR-182137 NASA, 1988.

[4] Reed, P.A.S., Wu, X.D., Sinclair, I. Fatigue crack path prediction in UDIMET 720 nickel-based alloy single crystals. Metallurgical and Materials Transactions A 2000;31A:109-123.

[5] Sih G. C., Paris P. C. and Irwin G. R. On cracks in rectilinearly anisotropic bodies. International Journal of Fracture Mechanics 1965;1(3):189-203.

[6] Snyder M. D. and Cruse T. A. Boundary-integral equation analysis of cracked anisotropic plates. International Journal of Fracture 1975;11 315-328.

[7] Labossiere, P.E.W., Dunn, M.L. Calculation of stress intensities at sharp notches in anisotropic media. Engineering Fracture Mechanics 1998;61:635-654.

[8] Zhao, J., Wu, X., Liu, R., Zhang, Z. Finite element analysis of a notch root semi-elliptical crack in single crystal superalloy. Engineering Fracture Mechanics 2004;71:1873-1890.

[9] Courtin, S., Gardin, C., Bezine, G., Ben Hadj Hamouda, H. Advantages of the J-integral approach for calculating stress intensity factors when using the commercial finite element code ABAQUS. Engineering Fracture Mechanics 2005;72:2174-2185.

[10] Timbrell, C., Chandwani, R. and Cook, G. State of the art in crack propagation, Les méthodes de dimensionnement en fatigue, Journée scientifique du 27 octobre 2004.

[11] Sha, J.B., Sun, J., Deng, Z.J., Zhou, H.J. Micro-crack tip fracture of commercial grade aluminium under mixed mode loading. Theoretical and Applied Fracture Mechanics 1999;31:119-130.

[12] Pickard, A. C. The application of 3-dimensional finite element methods to fracture mechanics and fatigue life prediction. London: Chameleon Press Ltd., 1986.

[13] Rooke, D. P. and Cartwright, D. J. Compendium of Stress Intensity Factors. Uxbridge: The Hillingdon Press, 1976.

[14] Tada, H., Paris, P. C., and Irwin, G. R. The stress analysis of cracks handbook. St. Louis: Del Research Corporation, 1973.

[15] Tinga, T. Automatic Stress Intensity Factor calculation using FE methods. Method development and user manual. NLR-CR-2003-568 Amsterdam: National Aerospace Laboratory, 2003.

[16] Mom, A. J. A. and Raizenne, M. D. AGARD engine disc cooperative test programme. Report no. 766 AGARD, 1989.

[17] Parekh, J.C., Arnold, R.R. and Woytowitz, P.J. A modern family of crack tip elements for MSC/Nastran. Universal City: MSC.Nastran user's conference, 1986.

[18] Kolkman, H. J. and Schra, L. Netherlands contribution to the TA31+/CARAD programme; Fatigue crack growth behaviour of single crystal alloy CMSX4. NLR-CR-2003-472 Amsterdam: National Aerospace Laboratory, 2003.